SAND2008-4305C

VHF and UHF Mechanically Coupled Aluminum Nitride MEMS Filters

Roy H. Olsson III, Cody M. Washburn, James E. Stevens, Melanie R. Tuck and Christopher D. Nordquist
Advanced MEMS Department
Sandia National Laboratories
Albuquerque, USA
rholsso@sandia.gov

***Abstract*—This paper reports the development of narrow-bandwidth, post-CMOS compatible aluminum nitride (AlN) MEMS filters operating in the very (VHF) and ultra (UHF) high frequency bands. Percent bandwidths less than 0.1% are achieved utilizing a mechanically coupled filter architecture, where a quarter wavelength beam attached in low velocity coupling locations is used to connect two AlN ring resonators. The filter bandwidth has been successfully varied from 0.09% to 0.2% by moving the attachment of the coupling beam on the ring to locations with different velocity at resonance. Insertion losses of 11 dB are obtained for filters centered at 99.5 MHz with low termination impedances of 200 Ω. Utilizing a passive temperature compensation technique, the temperature coefficient of frequency (TCF) for these filters has been reduced from -21 ppm/C to 2.5 ppm/C. The reduced TCF is critical for narrow bandwidth filters, requiring only 13% of the filter bandwidth to account for military range (-55 to 125 C) temperature variations compared to 100% for uncompensated filters. Filters operating at 557 MHz are realized using overtone operation of the ring resonators and coupling beam where higher insertion losses of 32 dB into 50 Ω are seen due to the finite resonator quality factor and narrow bandwidth design. Overtone operation allows for the implementation of fully differential and balun type filters where the stop-band rejection is as high as 38 dB despite the increased insertion loss.**

I. Introduction

Due to their high-Q, small size and ability to realize high selectivity filter banks covering multiple frequency bands (1 MHz to several GHz) directly on top of an integrated circuit, micromechanical filters are a promising technology for the miniaturization of high performance transceivers, multi-channel radios and real-time spectrum analyzers. Recently, piezoelectric aluminum nitride (AlN) micromechanical resonators [1-3], filters [3-8] and filter banks [3,4] have been developed that have lower motional impedance and higher power handling than capacitively transduced microresonator devices [9]. Utilizing a mechanically coupled filter architecture first reported for capacitively transduced ring resonators [10], this paper presents the design and characterization of high frequency selectivity AlN MEMS filters that achieve narrower percent bandwidths than previously reported filter architectures [3-8]. Given the small fractional bandwidths, this paper also addresses the temperature stabilization of AlN MEMS filters. Utilizing a thin oxide layer under the AlN filter film stack, the temperature stability has been improved from -21 ppm/C (parts-per-million per degrees C) to 2.5 ppm/C, making possible the application of these filters across the military temperature range (-55 to 125 C). The practical limitations of this temperature compensation technique are also presented and are expected to result in reproducible filters and resonators with 0.2 ppm/C temperature stability. Finally, mechanically coupled filters based on overtone operation are presented that achieve ultra-high frequencies (UHF) of 557 MHz. The higher than expected insertion losses of these UHF filters are determined to result from lower than expected resonator quality factors, Q, due anchor losses. Despite degraded resonator Q of 495, 0.1% bandwidth filters with 38 dB of stop-band rejection are obtained. The high stop-band rejection is a result of a fully differential filter design that is enabled by the overtone operation.

II. Fabrication Process and Temperaure Compensation

Pictured in Fig. 1 is the cross-section of an AlN composite microresonator showing the metal electrodes and AlN piezoelectric layer used to transduce the device and an oxide layer used for substrate isolation and temperature compensation. The highly c-axis oriented AlN piezoelectric layer with a rocking curve full-width-half-maximum less than 1.5° obtains strong electro-acoustic coupling that is used to obtain low insertion loss filters in a small die area. When a voltage is applied to the input electrodes across the piezoelectric layer, the bottom electrode is held at ground, an acoustic displacement is generated in the composite structure through the d_{31} piezoelectric coefficient as shown in Fig. 1. The stress induced in the AlN film by the acoustic wave generates a time-varying charge on the output electrodes which is passed through a resistor to give the resonator or filter output voltage. A detailed description of the AlN

This work was supported by the Laboratory Directed Research and Development (LDRD) program at Sandia National Laboratories. Sandia National Laboratories is a multiprogram laboratory operated by the Sandia Corporation, Lockheed Martin Company, for the United States Department of Energy's National Nuclear Security Administration under contract DE-AC04-94AL85000.

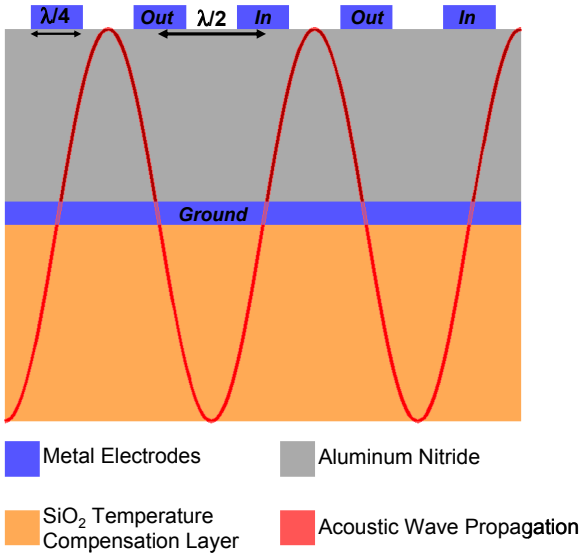

Figure 1. Cross-section of an AlN compsite microresonator with a SiO_2 temperature compensation layer.

microresonator fabrication process and operation is given in [1,3].

The AlN resonators and filters reported in [3] utilized a 400 nm oxide layer beneath the devices to provide isolation of the bottom electrode traces from the Si substrate. Resonators realized using this process have demonstrated a linear temperature coefficient of frequency (TCF) of -21 ppm/C, primarily induced by the negative temperature coefficient (TC) of Young's modulus for AlN. If left uncompensated this would result in nearly a 4000 ppm or 0.4% shift in frequency for resonators and filters implemented in this process across the military temperature range. Since the goal of this work is to realize narrow fractional bandwidth filters in the range of 0.1%, the TCF of previously reported AlN filters [6-8] must be improved to enable practical application of these devices. Recently, the positive TC of Young's modulus of SiO_2 has been used to compensate for the negative TC of Young's modulus in Si double ended tuning fork [11] and lateral bulk acoustic mode [12] resonators, resulting in orders of magnitude improvement in the frequency stability across temperature. Further investigation of Fig. 1 suggests that this technique should be easily applied to the AlN microresonator process reported in [3] by properly adjusting the thickness of the SiO_2 electrical isolation layer.

The TCF of AlN microresonators is primarily due to the change in sound velocity, $C_{effective}$, in the composite material over temperature, where the resonant frequency is given by

$$f(T) = \frac{C_{effecitve}(T)}{\lambda}. \quad (1)$$

The wavelength, λ, is used to lithographically set the resonance frequency of each resonator or filter and its temperature dependence is negligible compared to that of the sound velocity in an uncompensated structure. The sound velocity in the composite is equal to

$$C_{effective}(T) = \sqrt{\frac{\mathrm{E}_{effecitve}(T)}{\rho_{effective}}}, \quad (2)$$

where $E_{effective}$ and $\rho_{effective}$ are the effective Young's modulus and density of the composite resonator layer stack. When the thickness of the resonator is much less than the wavelength, which is the case for this work, the effective modulus and density can be accurately estimated using the following equations,

$$\mathrm{E}_{effective}(T) = \frac{\mathrm{E}_{AlN}(T)t_{AlN} + \mathrm{E}_{SiO_2}(T)t_{SiO_2} + \mathrm{E}_{Al}(T)t_{Al}}{t_{AlN} + t_{SiO_2} + t_{Al}} \quad (3)$$

$$\rho_{effective} = \frac{\rho_{AlN}t_{AlN} + \rho_{SiO_2}t_{SiO_2} + \rho_{Al}t_{Al}}{t_{AlN} + t_{SiO_2} + t_{Al}}, \quad (4)$$

where E, ρ, and t are the Young's modulus, density, and thickness of the material layers that comprise the composite resonator. From (1-3), since SiO_2 has a positive TC of Young's modulus while AlN and Al have a negative TC of Young's modulus, properly setting the thicknesses of these material layers will give a composite sound velocity and device resonance frequency that is independent of temperature to first order.

III. Mechanically Coupled Filter Architecture

Increasing the frequency selectivity of a filter or filter bank can result in improved transceiver sensitivity and dynamic range and more precise spectral analysis. Since many communications systems utilize channel bandwidths less than 100 kHz, the goal of this work is to minimize the fractional bandwidth of IF filters in the VHF and UHF bands as much as possible to improve system performance. Shown in Fig. 2 is a SEM image of a 99.5 MHz, 4th order mechanically coupled AlN MEMS filter. This filter architecture was first reported in [10] for capacitively transduced resonators and has demonstrated very narrow fractional bandwidths. For the piezoelectric implementation in Fig. 2, the drive resonator is electrically driven to expand and contract across the width of

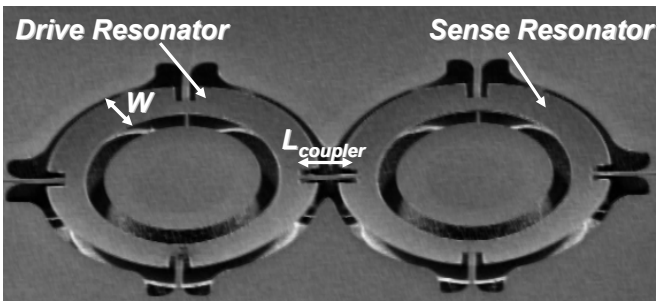

Figure 2. SEM image of a 4th order mechnaically-coupled AlN micro-filter.

the ring and the two poles of the filter are formed by the sense resonator vibrating either in or out of phase with the drive as shown in Fig. 3. The width of each ring, *W*, is 40 µm, corresponding to λ/2 at 99.5 MHz, where λ is the wavelength at resonance, and the rings are coupled by a 60 µm beam corresponding to a length of 3λ/4. Connecting the coupling beam to each ring at the lowest velocity location, the ring center, results in the narrowest possible bandwidth for the filter. By moving the coupling beam attachment to higher velocity locations, 2 µm, 4 µm and 6 µm offset from the ring center, the bandwidth of the filter can be increased. This is shown in Fig. 4 for coupling beam attachments (a) at the center of the ring and (b) 4 µm offset from the ring center.

The operation of the mechanically coupled filter in Fig. 2 can be extended to higher frequencies using overtone operation of the ring, as demonstrated for the 5th overtone filter shown in Fig. 5. In [3] it was demonstrated that by properly pattering the top metal electrode, overtones of the same ring resonator can be selectively driven while maintaining a constant Q and motional impedance even as the frequency is increased to nearly 700 MHz. Overtone operation also allows for the realization of fully differential or balun type filters that improve the rejection of out-of-band signals and increase device functionality.

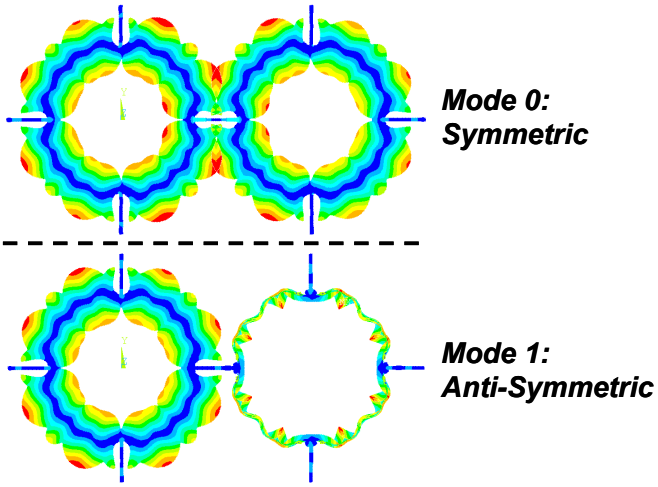

Figure 3. Symetric and anti-symmetric mode shapes that comprise the mechnanically coupled filter in Fig. 2.

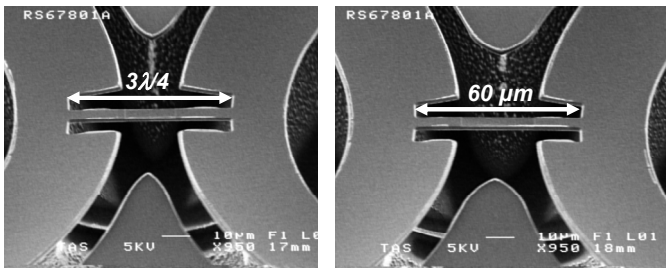

a) Low Velocity Coupling at Ring Center

b) Higher Velocity Coupling at 4 µm Offset from Ring Center

Figure 4. SEM images of the coupling locations for the AlN MEMS filter in Fig. 2, a) for low velocity, narrow bandwidth, coupling at the center of the ring and b) for higher velocity, higher bandwidth, coupling at 4 µm offset from the ring center.

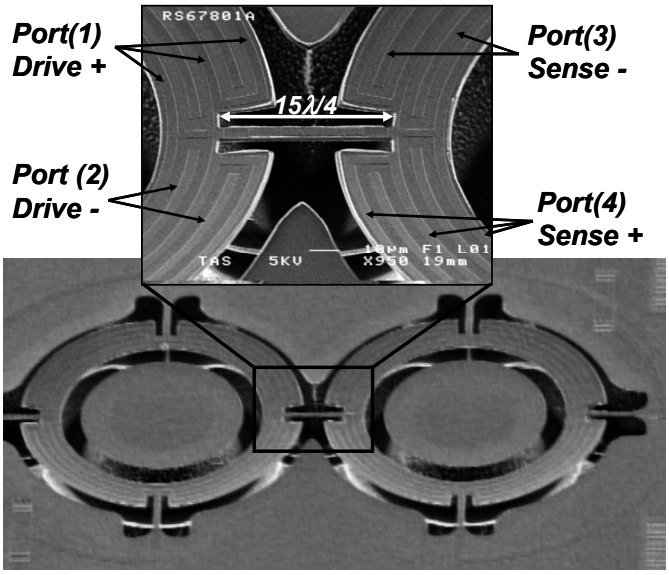

Figure 5. 5th overtone mechanically coupled filter SEM. Overtone design allows for single ended (2-port), balun (3-port) and fully differential (4-port) operation.

IV. Measured Results and Discussion

To evaluate the temperature compensation technique described above and to experimentally determine both the material properties of each layer in the composite resonator stack and the optimum oxide thickness to yield zero TCF, composite resonators with varying oxide thicknesses were fabricated. In all devices the AlN thickness was 750 nm and the total top and bottom metal thickness was 220 nm. Varying oxide thicknesses of 400, 650, 900, and 1150 nm were fabricated. The response of a single ring resonator similar to those pictured in Fig. 2 for each oxide thickness was measured over half the military temperature range (35 to 125 C) with the results shown in Fig. 6. Since the additional oxide thickness reduces the resonant frequency by up to 5%, the results in Fig. 6 are normalized to a frequency of 100 MHz at 35 C. As expected, increasing the oxide thickness initially results in a lower negative TCF for the ring resonators and eventually the TCF becomes positive for resonators with a 1150 nm oxide. Overall, the TCF is reduced from -21 ppm/C to 2.5 ppm/C, resulting in an order of magnitude higher temperature stability

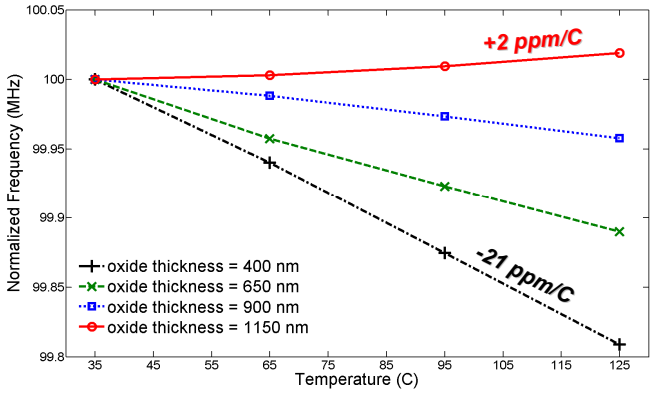

Figure 6. TCF for AlN ring resonators with different temperature compensation oxide thicknesses.

TABLE I. PERFORMANCE OF 100 MHZ ALN RING RESONATORS WITH VARYING TEMPERATURE COMPENSATION OXIDE THICKNESSES

Oxide Thickness (nm)	F_S (MHz)	F_P (MHz)	I.L. (dB)	Q	k_t^2 (%)	FOM (k_t^2Q)	TCF (ppm/C)
650	105.77	105.91	11.1	1440	0.33	4.8	-11.2
900	103.44	103.58	11.1	1527	0.32	4.9	-5.11
1150	102.85	103.07	8.8	1580	0.54	8.5	+2.49

critical for narrow fractional bandwidth filters. Shown in Table I are the measured critical performance parameters for the AlN ring resonators with different oxide thicknesses, where F_S, F_P, *I.L.*, Q, k_t^2, *FOM*, and *TCF* are the series resonant frequency, parallel resonant frequency, insertion loss, mechanical quality factor, coupling coefficient, figure of merit (k_t^2*Q) and temperature coefficient of frequency, respectfully. It should be noted that the resonators with 1150 nm oxide thickness required the development of a special vertical sidewall oxide etch to prevent multiple resonances from forming. This may account for the superior performance when compared to the devices with 650 and 900 nm thick oxides which were otherwise identically processed. From Table I no definitive statements can yet be made about the impact of the additional oxide thickness except that its effect is minimal over the range explored here. From the measured results a -67 ppm/C and +195 ppm/C TC of Young's modulus for AlN and SiO_2 can be extracted which is consistent with results found in the literature [1,11]. An optimum oxide thickness of 1060 nm can be determined with a predicted resonator TCF of 0.04 ppm/C. Since the compensation technique is dependant on maintaining a proper thickness ratio between the films, this level of temperature stability will not be repeatable over process variations. The thickness control of the thermal temperature compensation oxide in Fig. 1 is better than 0.1%. The 1 sigma thickness control, however, for the sputtered AlN film is 0.23% wafer-to-wafer and 1% across a 6 inch wafer. Given this level of thickness control, the predicted limits of this temperature compensation technique from (1-3), 1 sigma, are ±0.2 ppm/C or ±18.6 ppm across the military temperature range.

Fundamental mode mechanically coupled filters, shown in Fig. 2, with 1150 nm temperature compensation oxide thicknesses have been characterized. The filters were measured in air on a probe station where an optimum termination impedance of 200 Ω was found. Filters mechanically coupled at the center of the ring (lowest velocity coupling) and at 2, 4, and 6 µm offset from the ring center were characterized with the measured performance summarized in Table II. Shown in Fig. 7 are the measured responses for filters coupled at the ring center (narrowest bandwidth) and at 6 µm offset from the ring center (widest

TABLE II. MECHANICALLY COUPLED ALN FILTER PERFORMANCE

Ring Coupling Location	Center Frequency (MHz)	% Band-width	Insertion Loss (dB)	Stop-Band Rejection	20 dB Shape Factor
Center	99.5	0.09	11	39	3.8
2 µm offset	99.6	0.09	12	38	3.8
4 µm offset	99.6	0.11	11	39	3.3
6 µm offset	99.6	0.19	13	37	2.4

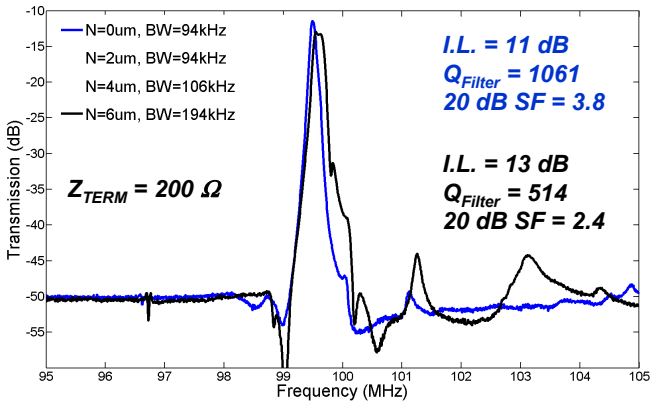

Figure 7. Measured response of the mechanically coupled filter in Fig. 2 for low velocity coupling at the center of the rings (Blue) and higher velocity coupling 6 µm offset from the ring center (Black). Higher velocity coupling increases the bandwidth by greater than a factor of 2.

bandwidth). The filters are centered at 99.5 MHz and the fractional bandwidth is varied from 0.09% to 0.19% by moving to higher velocity coupling locations. To our knowledge, these are the narrowest fractional bandwidth AlN MEMS filters reported to date.

To evaluate the effect of the oxide temperature compensation technique on filter thermal stability, filters mechanically coupled at 6 µm offset from the ring center with 1150 nm, Fig. 8, and 400 nm, Fig. 9, thick temperature compensation oxides were characterized from 35-125 C. 50 Ω termination impedances were used during all the temperature measurements. The results in Figs. 8 and 9 are very telling. Filters with 1150 nm temperature compensation oxides have a useable bandwidth of 181 kHz across the measured temperature range. This corresponds to 93.3% of the 194 kHz total filter bandwidth, where 6.7% of the filter bandwidth must be used to account for temperature variations. Filters from the process reported in [3] with 400 nm oxide thicknesses drift completely out of band across the measured temperature range. Clearly, without temperature compensation these narrow bandwidth filters would not be useful across the military temperature range. The temperature stability results

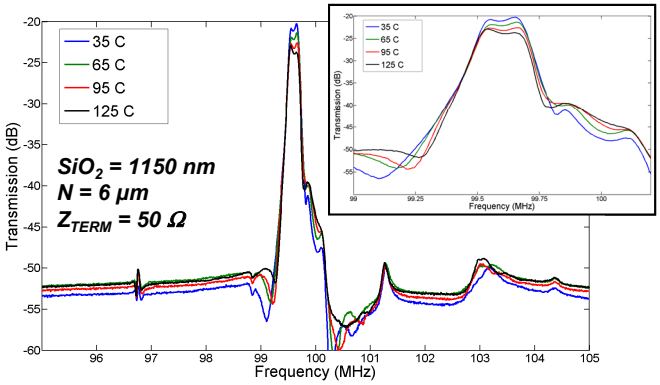

Figure 8. Measured response from 35 to 125 C of a temperature compensated AlN MEMS filter, Fig. 2, with high velocity mechanical coupling 6 µm from the ring center. Inset shows close-up of filter pass band. Only 6.7% of the filter bandwidth is needed to acount for varations over half of the military temperature range.

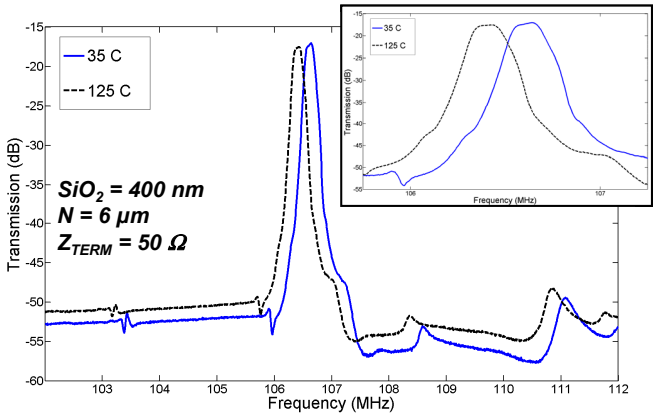

Figure 9. Measured response from 35 to 125 C of an uncompensated AlN MEMS filter with high velocity mechanical coupling 6 µm from the ring center. Inset shows close-up of filter pass band. Without compenation the filter drifts out of band across the required temperature range.

reported here cover only half of the military temperature range. Characterization below room temperature was limited due to condensation formed on the filter devices. This problem should be mitigated by a wafer level filter package currently under development. If the linear TCF results shown in Fig. 6 hold for temperatures below 25 C, only 13% of the filter bandwidth will be needed to account for military temperature variations for filters with fractional bandwidths below 0.2%. The increased insertion loss for this filter at higher temperatures, which is not seen in other co-fabricated AlN resonator and filter designs, should also be investigated in order to insert this device into an actual system.

The 5th overtone mechanically coupled filter shown in Fig. 5, with narrow bandwidth velocity coupling at the center of the rings, was evaluated experimentally on a probe station with the results presented in Fig. 10. A full 4-port characterization was performed on the filter in air with 50 Ω termination impedance. As can be seen in Fig. 10, the rejection of out-of-band signals is significantly improved when balun or fully differential operation is employed. The 32 dB filter insertion loss is much higher than predicted from previous results with overtone resonators reported in [3]. Utilizing the full 4-port measurement, the response of each individual resonator in the filter can also be evaluated, S21

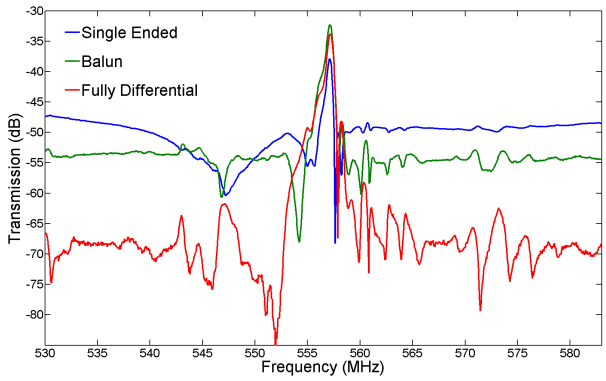

Figure 10. Measured response (2,3,and 4 port) of the 5th overtone mechancially coupled filter in Fig. 5. The coupling beams are attatched to low velcocity coupling locations at the ring center to give narrow bandwidth.

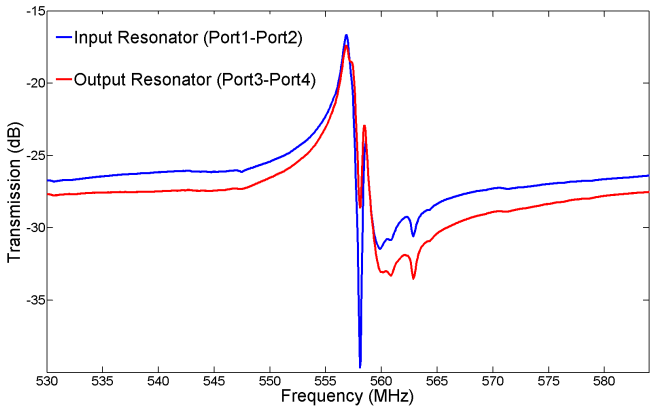

Figure 11. Measured response of the individual 5th overtone resonators that comprise the filter in Fig. 5. The Q's of these resonators are measured to be 495, half of that expected from [3] due to the doubling of the number of anchors. The finite resonator Q, which is half that for the filter, dramatically increases the filter insertion loss as shown in Fig. 10.

and S43 from Fig. 5, as shown in Fig. 11. In Fig. 11 it can be seen that the responses of the two resonators overlap in frequency and that the insertion loss is much lower than that for the filter. However, the Q of each resonator is only 495 while the filter Q is 1000, which leads to the much higher insertion loss. The 5th overtone ring resonators reported in [3] that demonstrated unloaded Q's of 1120 had only two anchors to the substrate while the resonators comprising the filter in Fig. 5 have four anchors. Since the Q is approximately halved here compared to the devices reported in [3], this suggests an anchor loss limited regime for the overtone ring resonators. Future overtone mechanically coupled filter designs based on 2-anchor ring resonators are expected to have significantly lower insertion loss.

V. Conclusions

Narrow fractional bandwidth, mechanically coupled AlN filters have been developed and characterized in the VHF and UHF frequency bands. Utilizing the low velocity coupling between two ring resonators, the bandwidth of low insertion loss, high power handling AlN MEMS filters has been reduced to less than 0.1%. A passive oxide temperature compensation technique has been demonstrated that reduces the TCF for AlN ring resonators to 2.5 ppm/C. When applied to the mechanically coupled filters, this temperature stabilization method requires only 13% of the filter bandwidth to be used to account for military temperature variations despite the narrow fractional bandwidths less than 0.2%. VHF implementations of these filters at 99.6 MHz have insertion losses of approximately 11 dB into 200 Ω and lithographically defined bandwidths based on velocity coupling from 0.09 to 0.2%. When scaled to UHF frequencies at 557 MHz, the 1st generation filters show high insertion loss because the filter bandwidth, 0.1%, is narrower than that of the resonators comprising the filter, 0.2%. Much lower insertion losses should be achieved in future UHF filter designs based on 2, rather than 4, anchor AlN ring resonators.

ACKNOWLEDGMENT

The authors would like to thank the Microelectronics Development Laboratory staff at Sandia National Laboratories including Todd Bauer, Rob Jarecki and Craig Nakakura for their work continuing to improve the AlN resonator process.

REFERENCES

[1] G. Piazza, P. J. Stephanou, and A. P. Pisano, "Piezoelectric aluminum nitride vibrating contour-mode MEMS resonators," *Journal of Microelectromechanical Systems,* vol. 15, no. 6, pp 1406-1418, Dec. 2006.

[2] D. J. D. Carter, J. Kang, D. White and A. E. Duwel, "Fabrication and measurement of an IC-compatible GHz-range piezoelectric longitudinal bar resonator," *Proc. of the Solid-State Sensor, Actuator, and Microsystems Workshop,* pp. 254-257, June 2004.

[3] R. H. Olsson III, J. G. Fleming, K. E. Wojciechowski, M. S. Baker and M. R. Tuck, "Post-CMOS compatible aluminum nitride MEMS filters and resonant sensors," *Proc. of the IEEE Frequency Control Symposium*, pp. 412-419, June 2007.

[4] R. H. Olsson III and M. R. Tuck, "Fundamental and overtone aluminum nitride dual mode resonator filters," *Proc of the Solid-State Sensor, Actuator, and Microsystems Workshop*, pp. 356-359, June 2008.

[5] K. E. Wojciechowski, R. H. Olsson III and M. R. Tuck, "Post-CMOS compatible aluminum nitride ring wave guide (RWG) resonators," *Proc. of the Solid-State Sensor, Actuator, and Microsystems Workshop*, pp. 372-375, June 2008.

[6] P. J. Stephanou, G. Piazza, C. D. White, M. B.J. Wijesundara and A. P. Pisano, "Piezoelectric aluminum nitride MEMS annular dual contour mode filter," *Sensors and Actuators A,* vol. 134*,* pp. 152-160, June 2006.

[7] G. Piazza, P. J. Stephanou, and A. P. Pisano, "Single-chip multiple frequency ALN MEMS filters based on contour-mode piezoelectric resonators," *Journal of Microelectromechanical Systems,* vol. 16, no. 2, pp. 319-328, April 2007.

[8] P. J. Stephanou, G. Piazza, C. D. White, M. B. J. Wijesundara and A. P. Pisano, "Mechanically coupled contour mode piezoelectric aluminum nitride MEMS filters," *Proc. of the IEEE International Conference on Microelectromechanical Systems*, pp. 906-909, Jan. 2006.

[9] C. T.-C. Nguyen, "MEMS technology for timing and frequency control," *IEEE Trans. on Ultrasonics, Ferroelectrics, and Frequency Control,* vol. 54, no. 2, pp. 251-270, Feb. 2007.

[10] S.-S. Li, Y.-W. Lin, Y. Xie, Z. Ren, and C. T.-C. Nguyen, "Small percent bandwidth design of a 431-MHz notch-coupled micromechanical hollow-disk ring mixer-filter," *Proc. of the IEEE International Ultrasonics Symposium*, pp. 1295-1298, Sept. 2005.

[11] R. Melamud, B. Kim, M. A. Hopcroft, S. Chandorkar, M. Agarwal, C. M. Jha and T. W. Kenny, "Composite flexural-mode resonator with controllable turnover temperature," *Proc. of the IEEE International Conference on Microelectromechanical Systems*, pp. 199-202, Jan. 2007.

[12] R. Abdolvand, H. Mirilavsani and F. Ayazi, "A low-volatge temperature-stable micromechanical piezoelectric oscillator" *Proc. of the IEEE International Confercence on Solid-State Sensors, Actuators and Microsystems (Transducers),* pp. 53-56, June 2007.